



ChemComm

Aromatic Hydroxylation of Anthracene Derivatives by a Chromium(III)-Superoxo Complex via Proton-Coupled Electron Transfer

Journal:	<i>ChemComm</i>
Manuscript ID	CC-COM-04-2019-003245.R1
Article Type:	Communication

SCHOLARONE™
Manuscripts

Aromatic Hydroxylation of Anthracene Derivatives by a Chromium(III)-Superoxo Complex *via* Proton-Coupled Electron Transfer†

Received 00th October 2016,
Accepted 00th January 20xx

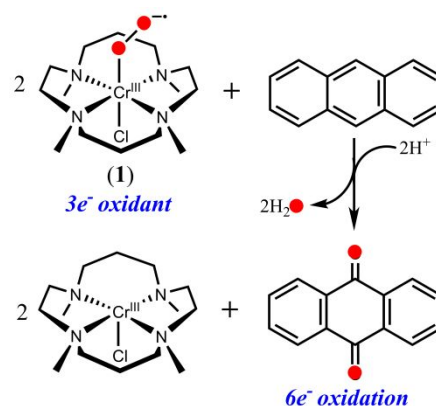
Tarali Devi,^a Yong-Min Lee,^a Wonwoo Nam,^{*a} and Shunichi Fukuzumi^{*ab}

DOI: 10.1039/x0xx00000x

www.rsc.org/

The chemistry of metal-superoxo intermediates started being unveiled in oxidation reactions by enzymes and their synthetic model compounds. However, aromatic hydroxylation reactions by the metal-superoxo species have yet to be demonstrated. In this study, we report for the first time that the hydroxylation of aromatic compounds such as anthracene and its derivatives by a mononuclear nonheme Cr(III)-superoxo complex, [(Cl)(TMC)Cr^{III}(O₂)]⁺ (**1**), occurs in the presence of triflic acid (HOTf) *via* the rate-determining proton-coupled electron transfer (PCET) from anthracene to **1**, followed by a fast further oxidation to give anthraquinone. The rate constants of electron transfer from anthracene derivatives to **1** in the presence of HOTf are well analyzed in light of the Marcus theory of electron transfer.

Metal-superoxo species have been proposed as the foremost intermediate generated during dioxygen activation process by the reduced metal centres in both heme and nonheme metalloenzymatic systems.¹⁻³ The intermediates have also been invoked as active oxidants in the C-H bond activation of organic substrates by nonheme enzymes containing iron (e.g., isopenicillin *N* synthase, *myo*-inositol oxygenase, 2-hydroxyethylphosphonate dioxygenase) and copper (e.g., dopamine β -monooxygenase, tyramine β -monooxygenase).⁴ In succession to metal-superoxo species, metal-(hydro)peroxo and metal-oxo species are also proposed to be generated during substrate oxygenation *via* dioxygen activation in natural and model systems.⁵⁻⁷ From the last few decades the high-valent metal-oxo species have been intensively investigated in a variety of oxidation reactions in heme and nonheme systems.⁸ However, efforts have also been made by the bioinorganic and biomimetic communities recently to explore the chemistry of metal-superoxo intermediates. Thus, successful



Scheme 1 Schematic representation of oxidation of anthracene by [(Cl)(TMC)Cr^{III}(O₂)]⁺ (**1**) in the presence of triflic acid (HOTf).

isolation and characterization of a number of metal-superoxo intermediates have been achieved in model systems⁹ and their reactivity studies have been examined towards electrophilic hydrogen atom transfer (HAT), oxygen atom transfer (OAT), hydride transfer and nucleophilic aldehyde deformylation reactions.¹⁰ It has also been reported very recently that chemical properties of the metal-superoxo species can be tuned by the presence of acid.¹¹ Although advances have been made in understanding reactivities of metal-superoxo species, their chemical properties still need to be fully explored and yet to be understood in broad aspects.

Aromatic hydroxylation has been described as one of the most challenging chemical processes mediated by many metalloenzymes, including cytochromes P450 and nonheme iron mono- and dioxygenases for biotransformations of pharmaceuticals and other xenobiotics, and high-valent oxoiron(IV) species have been invoked as active oxidants in the aromatic hydroxylation reactions.¹² In biomimetic studies, high-valent metal-oxo species have shown reactivities in the aromatic hydroxylation reactions, and their mechanistic studies have also been investigated through a combined experimental and theoretical approach.¹³ However, to the best of our knowledge, no report is available for a metal-superoxo species capable of hydroxylating aromatic compounds in both heme and nonheme systems.

^a Department of Chemistry and Nano Science, Ewha Womans University, Seoul 03760, Korea. E-mail: wwnam@ewha.ac.kr, fukuzumi@chem.eng.osak-u.ac.jp

^b Faculty of Science and Engineering, Meijo University, Nagoya, Aichi 468-8502, Japan.

† Electronic Supplementary Information (ESI) available: Detailed experimental procedures, Tables S1 and S2, and Fig. S1-S10. See DOI: 10.1039/x0xx00000x

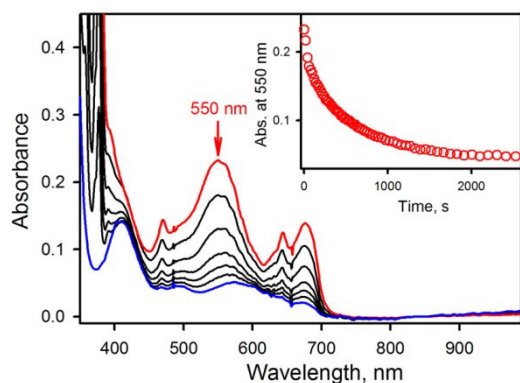


Fig. 1 UV-vis spectral changes observed in the 6-electron oxidation of anthracene (0.50 mM) by **1** (1.0 mM) in the presence of HOTf (1.0 mM) in MeCN at 233 K. The inset shows the time profile monitored at 550 nm due to the decay of **1**.

In biomimetic studies, a Cr(III)-superoxo complex, $[(\text{Cl})(\text{TMC})\text{Cr}^{\text{III}}(\text{O}_2)]^+$ (**1**; TMC = 1,4,8,11-tetramethyl-1,4,8,11-tetraazacyclotetradecane), was successfully synthesized and characterized spectroscopically and structurally. In addition, its reactivities towards hydrogen atom transfer (HAT), oxygen atom transfer (OAT) and hydride transfer reactions were reported as well.¹⁴ Very recently, it was also shown that the reactivity of **1** was remarkably enhanced towards OAT reactions in the presence of triflic acid (HOTf).¹¹ Such a remarkable enhancement of reaction rate in OAT reaction by **1** in the presence of HOTf was explained due to the much more positive shift of one-electron reduction potential of **1** ($E_{\text{red}} = 1.12 \text{ V vs. SCE}$) in the presence of HOTf (2.5 mM). As our ongoing efforts to elucidate detailed mechanistic insights of **1** into oxidation reactions, we have performed the reactivity study of **1** towards hydroxylation of aromatic compounds in the presence of HOTf. **1**, which was reported as a three-electron oxidant for the oxidation of NADH analogue,^{14c} can perform six-electron oxidation of anthracene to produce anthraquinone in the presence of HOTf under stoichiometric conditions in acetonitrile (MeCN) at 233 K. The mechanism of the proton-assisted hydroxylation of anthracene and its derivatives by **1** is clarified by comparison with the proton-coupled electron-transfer (PCET) reaction of **1** with one-electron donors in light of the Marcus theory of electron transfer. Thus, we believe that the present study provides a new scope to expand the reactivity of metal-superoxo species with HOTf as a hydroxylating agent of aromatic compounds.

Notably, the oxidation of anthracene by **1** does not occur in the absence of acid (*i.e.*, HOTf) in MeCN at 233 K (Fig. S1, ESI†). However, anthracene was fully oxidized (6-electron oxidation) by two equivalents of **1** (3-electron oxidant) in the presence of two equivalents of HOTf as shown in Fig. 1 (see also Scheme 1). The stoichiometry of the reaction was confirmed by UV-vis spectral titration experiments following the decay of absorption band at $\lambda_{\text{max}} = 550 \text{ nm}$ due to **1** upon addition of anthracene in the presence of HOTf in MeCN at 233 K (Fig S2, ESI†).

The product analysis after the reaction was performed by ¹H-NMR and GC-MS measurements, resulting that anthraquinone as six-electron oxidized product of anthracene was produced (Fig. S3 for NMR and Fig. S4 for GC-MS, ESI†). The yield of anthraquinone was found to be ~100% as analyzed with ¹H-NMR using cyclohexane as an internal reference. The source of oxygen in the anthraquinone product was confirmed by ¹⁸O-labeling experiment.

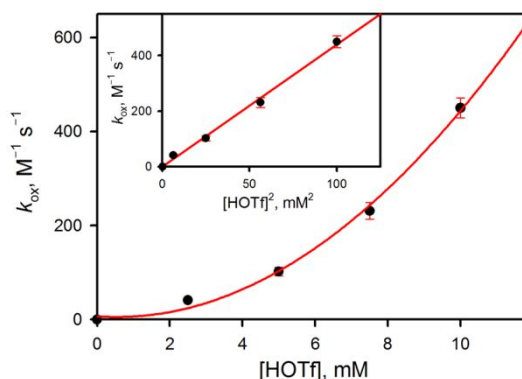


Fig. 2 Dependence of k_{ox} on $[\text{HOTf}]$ for the oxidation of anthracene (0.50 mM) by **1** (0.50 mM) in the presence of HOTf (0–10 mM) at 233 K. Inset shows the plot of k_{ox} vs. $[\text{HOTf}]^2$.

When the product obtained in the oxidation of anthracene by $\mathbf{1}\text{-}^{16}\text{O}_2$ ($[(\text{Cl})(\text{TMC})\text{Cr}^{\text{III}}(^{16}\text{O}_2)]^+$) in the presence of HOTf in MeCN at 233 K was compared with that obtained in the oxidation of anthracene by $\mathbf{1}\text{-}^{18}\text{O}_2$ ($[(\text{Cl})(\text{TMC})\text{Cr}^{\text{III}}(^{18}\text{O}_2)]^+$) in the presence of HOTf, peak at $m/z = 208$ for anthraquinone-¹⁶O,¹⁶O in GC-MS spectrum shifted to $m/z = 212$ for anthraquinone-¹⁸O,¹⁸O (Fig. S4 for GC-MS, ESI†), indicating that two oxygen atoms in anthraquinone originated from **1**. In addition, product analysis by CSI-MS and EPR measurements revealed that chromium(III) complex, $[\text{Cr}^{\text{III}}(\text{TMC})]^{3+}$ (**2**), was produced as the final inorganic product (Fig. S5, ESI†).

The kinetic measurements of the anthracene oxidation by **1** were performed by following the decay of absorbance at 550 nm due to **1** in the presence of HOTf (2.5 mM) in MeCN at 233 K. The decay rate of **1** in the oxidation of anthracene by **1** is given by eqn (1). According to the stoichiometry of the six-electron oxidation of anthracene by **1** (Scheme 1), the initial concentrations of **1** ($[\text{Cr}^{\text{III}}(\text{O}_2)]_0$) and anthracene ($[\text{An}]_0$) are given by eqns (2) and (3), respectively. Then, eqn (1) is rewritten by eqn (4).

$$-\text{d}[\text{Cr}^{\text{III}}(\text{O}_2)]/\text{d}t = k_{\text{ox}}[\text{Cr}^{\text{III}}(\text{O}_2)][\text{An}] \quad (1)$$

$$[\text{Cr}^{\text{III}}(\text{O}_2)]_0 = [\text{Cr}^{\text{III}}(\text{O}_2)] + [\text{Cr}^{\text{III}}] \quad (2)$$

$$[\text{An}]_0 = [\text{An}] + 2[\text{Cr}^{\text{III}}] \quad (3)$$

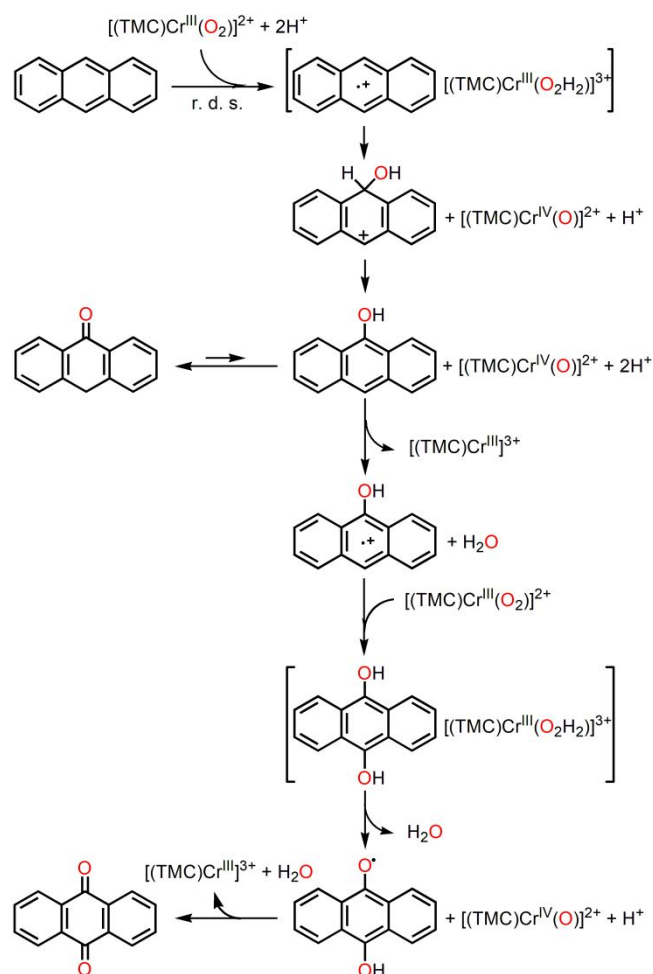
$$-\text{d}[\text{Cr}^{\text{III}}(\text{O}_2)]/\text{d}t = k_{\text{ox}}[\text{Cr}^{\text{III}}(\text{O}_2)]([\text{An}]_0 - 2[\text{Cr}^{\text{III}}(\text{O}_2)]_0 + 2[\text{Cr}^{\text{III}}(\text{O}_2)]) \quad (4)$$

Solving the differential eqn (4) with eqns (2) and (3) gives eqn (5)

$$\log[x/(C + 2x)] = -(C/2.3)k_{\text{ox}}t + \log[x_0/(C + 2x_0)] \quad (5)$$

where $x = [\text{Cr}^{\text{III}}(\text{O}_2)]$, $x_0 = [\text{Cr}^{\text{III}}(\text{O}_2)]_0$, $C = [\text{An}]_0 - 2[\text{Cr}^{\text{III}}(\text{O}_2)]_0$, $x_0/(C + 2x_0) = 1$. Thus, plot of $\log[x/(C + 2x)]$ vs. t gives a straight line that passes through zero with slope $= -(C/2.3)k_{\text{ox}}$, where C is $-x_0$. The k_{ox} value of the oxidation of anthracene by **1** in the presence of HOTf (2.5 mM) in MeCN at 233 K was determined by using eqn (5) to be $41(4) \text{ M}^{-1} \text{ s}^{-1}$ (Fig. S6 and Table S1, ESI†).

When anthracene was replaced by deuterated anthracene (anthracene-*d*₁₀), no kinetic isotope effect (KIE) was observed (Fig. S6, ESI†), suggesting that no C-H bond cleavage is involved in the rate-determining step. The reactivity of **1** towards oxidation of anthracene was further investigated varying HOTf concentration (Fig. S7, ESI†). The k_{ox} value of the oxidation of anthracene by **1** increased



Scheme 2. Plausible reaction mechanism.

with an increase in HOTf concentration (Fig. S8 and Table S1, ESI†), exhibiting second-order dependence with respect to HOTf concentration as shown in Fig. 2 [eqn (6)].¹⁵

$$k_{\text{ox}} = k_2[\text{HOTf}]^2 \quad (6)$$

Based on the results described above, the plausible mechanism of aromatic hydroxylation of anthracene by **1** in the presence of HOTf in MeCN at 233 K is shown in Scheme 2, where six-electron oxidation of anthracene by **1** in the presence of HOTf proceeds through the rate determining initial electron transfer from anthracene to **1** to produce anthracene radical cation and $[\text{Cr}^{\text{III}}(\text{TMC})(\text{O}_2\text{H}_2)]^{3+}$. Although the intermediates after the rate-determining step (r. d. s.) cannot be observed, the initial electron-transfer step may be followed by further oxidation of anthracene radical cation to generate 9-hydroxyanthracene and $[\text{Cr}^{\text{IV}}(\text{TMC})(\text{O})]^{2+}$ with the elimination of two protons. 9-Hydroxyanthracene is known to be tautomerized to anthrone,¹⁶ which is further oxidized by an electron transfer to the generated $[\text{Cr}^{\text{IV}}(\text{TMC})(\text{O})]^{2+}$ in the presence of two protons to produce 9-hydroxyanthracene radical cation and a $[\text{Cr}^{\text{III}}(\text{TMC})]^{3+}$ species.¹⁷ Further electron transfer takes place from 9-hydroxyanthracene radical cation to another molecule of **1** in the presence of water to generate 9,10-dihydroxyanthracene and $[\text{Cr}^{\text{III}}(\text{TMC})(\text{O}_2\text{H}_2)]^{3+}$. In the final step, anthraquinone is produced by stepwise electron transfer and

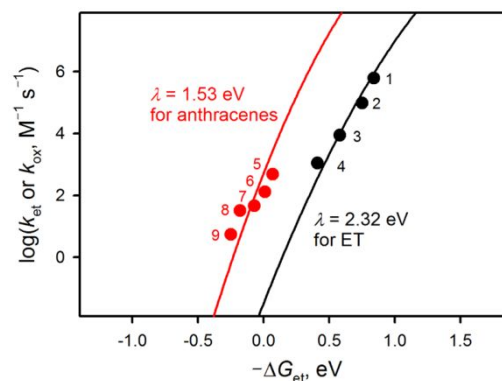


Fig. 3 Driving force ($-\Delta G_{\text{et}}$) dependence of rate constants ($\log k_{\text{et}}$ or $\log k_{\text{ox}}$) of electron transfer from ferrocene derivatives (black circles; (1) 1,1'-dimethylferrocene, (2) ferrocene, (3) bromoferrocene, (4) 1,1'-dibromoferrocene) and from anthracene derivatives (red circles; (5) 9,10-dimethylantracene, (6) 9-methylantracene, (7) anthracene (8) 9-bromoanthracene and (9) 9-anthracenecarboxaldehyde) to **1** in the presence of HOTf (2.5 mM) at 233 K. The red and black lines are Marcus lines calculated with λ values of 1.53 and 2.32 eV, respectively.

proton transfer from 9,10-dihydroxyanthracene to $[\text{Cr}^{\text{III}}(\text{TMC})(\text{O}_2\text{H}_2)]^{3+}$ to finally produce **2**, accompanied by the elimination of water.

The kinetic measurements for the oxidation of 9-substituted anthracene derivatives (XAn), such as 9-methylantracene, 9-bromoanthracene and 9-anthracenecarboxaldehyde, were also examined in the presence of HOTf (2.5 mM) in MeCN at 233 K. According to the stoichiometry of the four-electron oxidation of XAn by **1** (3-electron oxidant), the kinetic equations are derived to determine the second-order rate constant (k_{ox}) (see Experimental Section in ESI†; Determination of k_{ox} value for the four-electron oxidation of substrate by 3-electron oxidant). The k_{ox} values of the four-electron oxidation of XAn by **1** were determined by using eqn (S5) in ESI† (see also Fig. S10 and Table S2, ESI†).

The kinetic measurements for the oxidation of 9,10-dimethylantracene were also performed in the presence of HOTf (2.5 mM) in MeCN at 233 K. The second-order rate constants (k_{ox}) for the two-electron oxidation of 9,10-dimethylantracene by **1** (3-electron oxidant) was determined by using eqn (S10) in ESI† (see Experimental Section in ESI†; Determination of k_{ox} value for the two-electron oxidation of substrate by 3-electron oxidant; Fig. S11 and Table S2, ESI†).

The rate constants of proton assisted hydroxylation of anthracene and its derivatives by **1** is then compared with the rate constants of outer-sphere electron-transfer reactions as explained by the Marcus theory of electron transfer [eqn (7)].¹⁸

$$k_{\text{et}} = Z \exp[-(\lambda/4)(1 + \Delta G_{\text{et}}/\lambda)^2/(k_{\text{B}}T)] \quad (7)$$

where Z is the collision frequency which is normally taken as $1 \times 10^{11} \text{ M}^{-1} \text{ s}^{-1}$, which corresponds to $k_{\text{B}}TK/h$ (k_{B} is the Boltzmann constant, T is the absolute temperature, K ($\approx 0.020 \text{ M}^{-1}$)¹⁸ is the formation constant of the precursor complex, and h is the Planck constant), λ is the reorganization energy of electron transfer and ΔG_{et} is the free energy change of electron transfer. The driving force ($-\Delta G_{\text{et}}$) values were determined from the difference between the one-electron oxidation potentials (E_{ox}) of electron donors and the one-electron

reduction potential of **1** ($E_{\text{red}} = 1.12$ V vs. SCE) in the presence of HOTf (2.5 mM), as given by eqn (8), where e is the elementary charge.

$$-\Delta G_{\text{et}} = e(E_{\text{red}} - E_{\text{ox}}) \quad (8)$$

The driving force dependence of logarithm of the rate constants of outer-sphere electron transfer (k_{et}) from one-electron donors (*i.e.*, ferrocene derivatives) to **1** in the presence of HOTf (2.5 mM) in MeCN at 233 K is shown in Figure 3 (black circles), where the $\log k_{\text{et}}$ values¹¹ are plotted against the $-\Delta G_{\text{et}}$ values. The driving force dependence of k_{et} is well fitted by the black line in Figure 3 using eqn (7) with the λ value of 2.32 eV.¹¹ The rate constants of electron transfer from anthracene derivatives (k_{ox}) to **1** are also plotted against $-\Delta G_{\text{et}}$ values in Figure 3 (red circles), where the driving force dependence of k_{ox} is fitted with somewhat smaller reorganization energy of $\lambda = 1.53$ eV (red line in Fig. 3). The smaller λ value for the case of anthracene derivatives in the Marcus plot compared with that of outer-sphere electron transfer from one-electron donors (*i.e.*, ferrocene derivatives) to **1** may be accounted by much faster electron exchange between 9,10-dimethylantracene and 9,10-dimethylantracene radical cation ($5.0 \times 10^8 \text{ M}^{-1} \text{ s}^{-1}$)^{18a} compared to that between ferrocene and ferrocenium cation ($5.3 \times 10^6 \text{ M}^{-1} \text{ s}^{-1}$) in MeCN^{18b} and small bond reorganization energy of anthracene derivatives, which are delocalized π -compounds.^{12c}

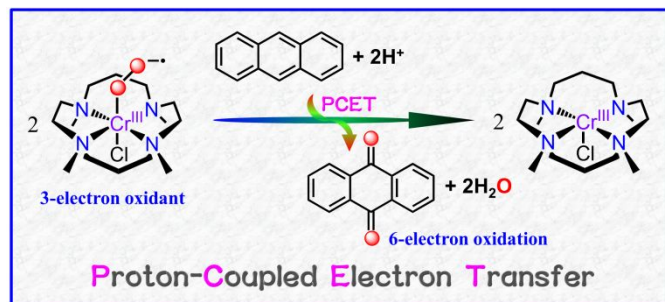
In conclusion, aromatic hydroxylation of anthracene by **1** has been made possible in the presence of HOTf to produce anthraquinone, which is the fully oxidized (six-electron oxidation) product of anthracene. The reaction proceeds *via* the rate-determining PCET from anthracene to **1**, followed by the subsequent fast oxidation reactions all the way to anthraquinone. In addition, no KIE (*i.e.*, KIE = 1) also suggests no involvement of C-H bond cleavage in the rate-determining step, which is PCET. The rates of PCET from anthracene derivatives to **1** were evaluated in comparison with the outer-sphere electron-transfer reactions from one-electron donors to **1** in the presence of HOTf in light of the Marcus theory of electron transfer. This study provides valuable mechanistic insight into the hydroxylation of aromatic substrates by metal-superoxo species *via* the rate-limiting PCET process.

This work was supported by a SENTAN project from Japan Science and Technology Agency (JST) to S.F. and JSPS KAKENHI (No. 16H02268 to S.F.) from MEXT, Japan, and the NRF of Korea through CRI (NRF-2012R1A3A2048842 to W.N.), GRL (NRF-2010-00353 to W.N.), and Basic Science Research Program (2017R1D1A1B03029982 to Y.-M.L. and 2017R1D1A1B03032615 to S.F.).

References

- (a) X. Huang and J. T. Groves, *Chem. Rev.*, 2018, **118**, 2491; (b) S. Sahu and D. P. Goldberg, *J. Am. Chem. Soc.*, 2016, **138**, 11410; (c) S. Hong, Y.-M. Lee, K. Ray and W. Nam, *Coord. Chem. Rev.*, 2017, **334**, 25; (d) W. Nam, *Acc. Chem. Res.*, 2015, **48**, 2415.
- (a) D. A. Quist, D. E. Diaz, J. J. Liu and K. D. Karlin, *J. Biol. Inorg. Chem.*, 2017, **22**, 253; (b) G. Yin, *Acc. Chem. Res.*, 2013, **46**, 483; (c) J. A. Kovacs, *Acc. Chem. Res.*, 2015, **48**, 2744.
- (a) A. Mukherjee, M. A. Cranswick, M. Chakrabarti, T. K. Paine, K. Fujisawa, E. Münck and L. Que, Jr., *Inorg. Chem.*, 2010, **49**, 3618; (b) S. Fukuzumi and K. D. Karlin, *Coord. Chem. Rev.*, 2013, **257**, 187.
- (a) C. E. Elwell, N. L. Gagnon, B. D. Neisen, D. Dhar, A. D. Spaeth, G. M. Yee and W. B. Tolman, *Chem. Rev.*, 2017, **117**, 2059; (b) W. A. van der Donk, C. Krebs and J. M. Bollinger, Jr., *Curr. Opin. Struct. Biol.*, 2010, **20**, 673; (c) J. J. Liu, D. E. Diaz, D. A. Quist and K. D. Karlin, *Isr. J. Chem.*, 2016, **56**, 738; (d) E. G. Kovaleva and J. D. Lipscomb, *Nat. Chem. Biol.*, 2008, **4**, 186; (e) J. M. Bollinger, Jr. and C. Krebs, *Curr. Opin. Chem. Biol.*, 2007, **11**, 151.
- (a) C.-C. Wang, H.-C. Chang, Y.-C. Lai, H. Fang, C.-C. Li, H.-K. Hsu, Z.-Y. Li, T.-S. Lin, T.-S. Kuo, F. Neese, S. Ye, Y.-W. Chiang, M.-L. Tsai, W.-F. Liaw and W.-Z. Lee, *J. Am. Chem. Soc.*, 2016, **138**, 14186; (b) T. Fujii, S. Yamaguchi, Y. Funahashi, T. Ozawa, T. Tosha, T. Kitagawa and H. Masuda, *Chem. Commun.*, 2006, 4428; (c) Y. M. Kim, K.-B. Cho, J. Cho, B. Wang, C. Li, S. Shaik and W. Nam, *J. Am. Chem. Soc.*, 2013, **135**, 8838.
- (a) J.-G. Liu, Y. Shimizu, T. Ohta and Y. Naruta, *J. Am. Chem. Soc.*, 2010, **132**, 3672; (b) R. Cao, C. Saracini, J. W. Ginsbach, M. T. Kieber-Emmons, M. A. Siegler, E. I. Solomon, S. Fukuzumi and K. D. Karlin, *J. Am. Chem. Soc.*, 2016, **138**, 7055.
- (a) D. Kumar, W. Thiel and S. P. de Visser, *J. Am. Chem. Soc.*, 2011, **133**, 3869; (b) Y.-M. Lee, S. Hong, Y. Morimoto, W. Shin, S. Fukuzumi and W. Nam, *J. Am. Chem. Soc.*, 2010, **132**, 10668; (c) J. Cho, J. Woo and W. Nam, *J. Am. Chem. Soc.*, 2012, **134**, 11112.
- (a) M. Guo, T. Corona, K. Ray and W. Nam, *ACS Cent. Sci.*, 2019, **5**, 13; (b) H. B. Gray and J. R. Winkler, *Acc. Chem. Res.*, 2018, **51**, 1850; (c) S. Fukuzumi, T. Kojima, Y.-M. Lee and W. Nam, *Coord. Chem. Rev.*, 2017, **333**, 44; (d) M. Puri and L. Que, Jr., *Acc. Chem. Res.*, 2015, **48**, 2443.
- (a) C.-W. Chiang, S. T. Kleespies, H. D. Stout, K. K. Meier, P.-Y. Li, E. L. Bomina, L. Que, Jr., E. Münck and W.-Z. Lee, *J. Am. Chem. Soc.*, 2014, **136**, 10846; (b) S. Hong, K. D. Sutherland, J. Park, E. Kwon, M. A. Siegler, E. I. Solomon and W. Nam, *Nat. Commun.*, 2014, **5**, 5440; (c) A. Kunishita, M. Kubo, H. Sugimoto, T. Ogura, K. Sato, T. Takui and S. Itoh, *J. Am. Chem. Soc.*, 2009, **131**, 2788; (d) M. T. Kieber-Emmons, J. Annaraj, M. S. Seo, K. M. Van Heuvelen, T. Tosha, T. Kitagawa, T. C. Brunold, W. Nam and C. G. Riordan, *J. Am. Chem. Soc.*, 2006, **128**, 14230.
- (a) M. Sankaralingam, Y.-M. Lee, W. Nam and S. Fukuzumi, *Coord. Chem. Rev.*, 2018, **365**, 41; (b) A. D. Ure and A. R. McDonald, *Synlett*, 2015, **26**, 2060.
- T. Devi, Y.-M. Lee, W. Nam and S. Fukuzumi, *J. Am. Chem. Soc.*, 2018, **140**, 8372.
- (a) C. M. Bathelt, L. Ridder, A. J. Mulholland and J. N. Harvey, *J. Am. Chem. Soc.*, 2003, **125**, 15004; (b) M. Asaka and H. Fujii, *J. Am. Chem. Soc.*, 2016, **138**, 8048; (c) N. Sharma, J. Jung, Y.-M. Lee, M. S. Seo, W. Nam and S. Fukuzumi, *Chem. Eur. J.*, 2017, **23**, 7125.
- (a) S. P. de Visser, K. Oh, A.-R. Han and W. Nam, *Inorg. Chem.*, 2007, **46**, 4632; (b) D. Kumar, G. N. Sastry and S. P. de Visser, *J. Phys. Chem. B*, 2012, **116**, 718.
- (a) J. Cho, J. Woo and W. Nam, *J. Am. Chem. Soc.*, 2010, **132**, 5958; (b) J. Cho, J. Woo and W. Nam, *J. Am. Chem. Soc.*, 2012, **134**, 11112; (c) T. Devi, Y.-M. Lee, J. Jung, M. Sankaralingam, W. Nam and S. Fukuzumi, *Angew. Chem. Int. Ed.*, 2017, **129**, 3564.
- (a) J. Park, Y. Morimoto, Y.-M. Lee, W. Nam and S. Fukuzumi, *J. Am. Chem. Soc.*, 2012, **134**, 3903; (b) Y. Morimoto, H. Kotani, J. Park, Y.-M. Lee, W. Nam and S. Fukuzumi, *J. Am. Chem. Soc.*, 2011, **133**, 403.
- H.-G. Korth and P. Mulder, *J. Org. Chem.*, 2013, **78**, 7674.
- It should be noted that, in the oxidation of anthracene by $[\text{Cr}^{\text{IV}}(\text{TMC})(\text{O})]^{2+}$ in the presence of HOTf at 233K, almost no reaction occurred (see Fig. S9, ESI†), indicating that $\text{Cr}(\text{III})$ -superoxo complex (**1**) is the actual reactive intermediate for the oxidation of anthracene.
- (a) R. A. Marcus, *Annu. Rev. Phys. Chem.*, 1964, **15**, 155; (b) R. A. Marcus and N. Sutin, *Biochim. Biophys. Acta, Rev. Bioenerg.*, 1985, **811**, 265; (c) R. A. Marcus, *Angew. Chem. Int. Ed. Engl.*, 1993, **32**, 1111; (d) J. Park, Y. Morimoto, Y.-M. Lee, W. Nam and S. Fukuzumi, *Inorg. Chem.*, 2014, **53**, 3618.
- (a) S. Fukuzumi, I. Nakanishi and K. Tanaka, *J. Phys. Chem. A*, 1999, **103**, 11212; (b) E. S. Yang, M.-S. Chan and A. C. Wahl, *J. Phys. Chem.*, 1980, **84**, 3094; (c) S. Fukuzumi, S. Mochizuki and T. Tanaka, *Inorg. Chem.*, 1989, **28**, 2459.

Table of Contents Graphic



Aromatic hydroxylation of anthracene by a mononuclear nonheme Cr(III)-superoxo complex proceeds *via* the rate-determining proton-coupled electron transfer, followed by fast further oxidation to anthraquinone.